Lawrence Berkeley Laboratory

UNIVERSITY OF CALIFORNIA

Presented at the 7th High Energy Heavy Ion Study,
GSI, Darmstadt, W. Germany, October 8-12, 1984

CLUSTER PRODUCTION AND ENTROPY

H.-Å. Gustafsson, K.G.R. Doss, H.H. Gutbrod, B. Kolb,
H. Löhner, B. Ludewigt, A.M. Poskanzer, T. Renner,
H. Riedesel, H.G. Ritter, A. Warwick, and H. Wieman

January 1985

NUCLEAR SCIENCE DIVISION

Prepared for the U.S. Department of Energy under Contract DE-AC03-76SF00098

LBL-18949

Cluster Production and Entropy

H.-Å. Gustafsson,[a] K.G.R. Doss,[b] H.H. Gutbrod,[a] B. Kolb,[a] H. Löhner,[a1] B. Ludewigt,[a2] A.M. Poskanzer,[b] T. Renner,[b] H. Riedesel,[b3] H.G. Ritter[a], A. Warwick[a4] and H. Wieman[a]

[a]Gesellschaft für Schwerionenforschung
D-6100 Darmstadt, West Germany

and

[b]Nuclear Science Division, Lawrence Berkeley Laboratory
University of California, Berkeley, California 94720

This work was supported in part by the Director, Office of Energy Research, Division of Nuclear Physics of the Office of High Energy and Nuclear Physics of the U.S. Department of Energy under Contract DE-AC03-76SF00098.

[1]Present address: Institut für Kernphysik, Universität Münster, D-4400 Münster West Germany

[2]Fachbereich Physik, Philipps Universität Marburg, D-3550 Marburg 1 West Germany

[3]Present address: Springer Verlag, Berlin West Germany

[4]Present address: Lawrence Berkeley Laboratory, University of California, Berkeley, CA 94720

LBL-18949

Cluster Production and Entropy

H.-Å. Gustafsson,[a)] K.G.R. Doss,[b)] H.H. Gutbrod,[a)] B. Kolb,[a)] H. Löhner,[a1)] B. Ludewigt,[a2)] A.M. Poskanzer,[b)] T. Renner,[b)] H. Riedesel,[b3)] H.G. Ritter[a)], A. Warwick[a4)] and H. Wieman[a)]

[a)] Gesellschaft für Schwerionenforschung
D-6100 Darmstadt, West Germany

and

[b)] Nuclear Science Division, Lawrence Berkeley Laboratory
University of California, Berkeley, California 94720

Introduction:

One of the ultimate goals in relativistic nuclear physics is to study the behavior of nuclear matter at densities different from the ground state density. It has been suggested that composite particle production [1,2,3,4] as well as two-particle correlations [1,5] are relevant observables to determine the size of the participant volume at freeze out. However, the two particle correlation method determines the thermal freeze out density, the

This work was supported in part by the Director, Office of Energy Research, Division of Nuclear Physics of the Office of High Energy and Nuclear Physics of the U.S. Department of Energy under Contract DE-AC03-76SF00098.

[1)] Present address: Institut für Kernphysik, Universität Münster, D-4400 Münster West Germany

[2)] Fachbereich Physik, Philipps Universität Marburg, D-3550 Marburg 1 West Germany

[3)] Present address: Springer Verlag, Berlin West Germany

[4)] Present address: Lawrence Berkeley Laboratory, University of California, Berkeley, CA 94720

density at which collisions between fragments cease, while the composite particle production method determines the chemical freeze out density, the density at which composite particles cease to form and break up. Furthermore, there are calculations [6,7,8] showing that the observed ratio of deuterons to protons can be related to the produced entropy in the system. If the entropy stays constant during the expansion phase [9,10], the composite particles contain information not only about the freeze out but also about the initial stage of the collision, where the nuclear matter is compressed and hot.

The importance of contributions from heavier fragments ($A > 4$) for the entropy production has been discussed [7,8]. Since the cross-section for producing heavy fragments goes down with increasing bombarding energy [8] this effect is most important at low bombarding energies while at higher energies the contribution is thought to be negligible. In addition there are also different suggestions [7,9] as to how the production of composite particles other than deuterons should be counted. Our results are of course dependent on the counting scheme used.

Experiment:

The experiments, studying 400 and 1050 MeV/nucleon Ca + Ca and 400 and 650 MeV/nucleon Nb + Nb, were carried out at the Berkeley Bevalac. The data were taken with the Plastic Ball/Wall spectrometer [11]. Fig. 1 shows a schematic view of the spectrometer. The Plastic Ball covers an angular range of 9 - 160 degrees in the laboratory system and the forward angular range from 0 - 9 degrees is covered by the Plastic Wall. This is in part also used to define the event trigger. The data presented here were taken using both a minimum bias trigger and a central collision trigger.

<u>Composite particle production</u>:

To extract information about the size and density of the participant volume, it is of great importance to exclude the target and projectile spectators in the analysis. It is equally important to cover approximately the same area in phase space when comparing the production rates for different species. The d/p ratio determines the volume of the system at freeze out and to determine the density one needs to know the number of baryons in this volume. We define N_p as the participant baryon charge multiplicity. It also takes into account the participant protons bound in clusters (d,t,^{3}He,^{4}He). That can easily contribute up to about 40 percent to N_p. To determine the participant multiplicity the spectator particles were removed by introducing software cuts in the analysis. In the target region a cut corresponding to 12 MeV/nucleon in the laboratory frame was introduced. This threshold corresponds roughly to the experimental cut off due to absorption in the target and in the walls of the scattering chamber. In the projectile region the spectator particles were eliminated by applying a cut in the $p_\perp$-rapidity plane.

The Plastic Ball has full particle identification only in a limited part of the full phase space. Therefore a model is needed to extrapolate from differentially measured to total integrated yields. Assuming the coalescence model to be valid one can determine the overlap region in phase space for the different species. This was done in the space where the particle momenta have been scaled by $(1/m)^{1/2}$, where m is the mass of the different species (p,d,t,^{3}He,^{4}He). This procedure follows directly from the formalism described in ref. 3.

Fig. 2 shows the yield of the d_{like}/p_{like} ratio in the overlap region as a function of N_p for Ca + Ca and Nb + Nb at different bombarding energies. The definitions of d_{like} and p_{like} were taken from ref. 9.

The functional form of the observed d_{like}/p_{like} ratios can be understood in terms of the coalescence model [1,4,12]. In this report we have used an improved version of the model [1] which is a complete 6 dimensional phase space calculation [3] relating the radii of the deuteron and the participant zone to the coordinate space, and relating the temperature of the interacting region to the momentum space. In this model the radius, r_p, and the temperature, T, of the interacting region as well as the deuteron radius, r_d, are related to d_{like} and p_{like} through

$$d_{like}/p_{like} = 6*((A - Z)/Z)*(1 + 2*(r_p/r_d)**2)^{-3/2} * N_p *$$

$$* (1 + 2*m*T*(r_d **2)/3)^{-3/2} \qquad (1)$$

where the factor (A - Z)/Z makes up for the difference between neutron and proton number and m is the nucleon mass. The radius r_o, assuming a spherical source is parameterized as $r_p = r_o *(A/Z * N_p)^{1/3}$, where A/Z is the factor converting the participant baryon charge multiplicity to participant baryon multiplicity. The reduced radius, r_o, is then related to the density by $\rho = 1/((4*\pi*r_0**3)/3)$. The formula for r_p differs from the one used in ref. 4 where r_p was related to $\tilde{p}_{like}$ which was twice the yield of proton-like particles determined in the backward hemisphere of the center of mass system. In this report r_p is related to N_p, which is a more accurate measure of the participant nucleons. The temperature entering formula (1) is the apparent

temperature obtained from particle spectra (one does not need to have a thermalized system or to know the true temperature which might be lower than the apparent one due to radial flow [13]). This is a first order approximation to the original full 6 dimensional phase space calculation [3] where both the parallel and longitudinal temperatures enter. In the fits to the observed ratios, r_o and r_d were free parameters. The temperature T was taken to be the mean temperature obtained from Boltzmann fits [13] to the proton spectra at 90 degrees in the center of mass system. The fits to the experimental ratios were done for $N_p > 5$ and the results are presented as solid curves in fig. 2. The temperatures used as well as the extracted parameters are given in Table 1. The r_o values in the table are the rms values for a Gaussian density distribution. To convert these values to equivalent sharp sphere radii the listed values have to be multiplied by $(5/3)^{1/2}$. The r_o^{ssp} values obtained for the four cases studied vary between 1.19 and 1.50 fm. The corresponding freeze out densities are shown in fig. 3a.

The extracted chemical freeze out densities between 0.5 and 1.0 times normal nuclear matter density deviate from the results obtained from two-particle correlations [14] which gives a thermal freeze out density of about 0.25 times normal nuclear matter density. Some possible explanations for this observed difference might be:

a) In the case of composite particle production which involves bound resonances a third particle has to be present to conserve momentum and energy while in the p-p correlation case involving unbound resonances a third particle is not necessary. Because of the necessary presence of the third

particle the chemical freeze out density determined from the d/p ratios ought to be higher than the thermal freeze out density extracted from the two-particle correlation analysis.

b) After the creation of the hot interaction zone it cools and expands. During this stage there are still interactions going on between the particles. The p-p correlations are easily disturbed by small interactions while the bound composite particles are much more immune, thus giving a higher chemical freeze out density than thermal freeze out density.

From fig. 2 it is seen that, when comparing the two systems at the same energy and number of participants, the production of composite particles is approximately the same. On the other hand when comparing the low energy data with the data at the higher energies it is seen that the production of heavier particle decreases with increasing bombarding energy. This is thought to be due to higher temperatures suppressing the production of composite particles.

Fig. 2 also shows that the d_{like}/p_{like} ratios increases with increasing proton multiplicity. One might interpret this as being an effect of finite particle number limiting the formation of composites. However, we did a calculation using a statistical model [15] modified to give a constant temperature as a function of impact parameter. It shows that the finite particle number effect vanishes already at multiplicities around $N_p = 5$ while the curves in fig. 2 continue to rise at much higher proton multiplicities before leveling off. This behavior can instead be interpreted as an effect of the finite size of the deuteron which, at low N_p, has less overlap with the small participant volume [4].

Entropy production for infinite nuclear matter:

There are different models relating the production of composite particles to the produced entropy in the system. We will here present the results extracted from our data using the models of Kapusta [7] and Stöcker [8] and will also briefly discuss the differences between these two methods. In our analysis the number of d_{like} and p_{like} particles are counted as in the definitions given in ref. 9.

Both models discussed here are calculations for infinite nuclear matter and use the asymptotic values for large N_p of the ratio, $(d_{like}/p_{like})_{asymp}$, to determine the produced entropy. The asymptotic values of the ratios were determined by using equation (1) for infinite proton multiplicity. With the parameters extracted from the fits shown in fig. 2 and given in Table 1, the asymptotic values were determined for all systems. These values were then used to extract the entropy per nucleon (S/A) in accordance to the two models.

The asymptotic values and the corresponding entropy values S/A obtained from the two models are given in Table 2. The errors given are based on the errors in the fit parameters due to statistics. Also shown are the d_{like}/p_{like} ratios at maximum charge baryon number (Z of the projectile plus the Z of the target). These values could be used to extract entropy for comparison with calculations for a finite nuclear system at zero impact parameter.

Both models are quantum-statistical calculations including the effect of the finite volume of the particles. The model of Kapusta [7] predicts the number of real deuterons and deuteron-pairings contained in heavier clusters but it does not say what these clusters are. The model of Stöcker [8] (see

also fig. 6 in ref. 16). includes the production of heavy clusters up to A = 20 as well as the decay of all unbound resonances for these species. This model also includes the contribution to the entropy from the production of pions and deltas, while in the model of Kapusta [7] these are not taken into account. The contribution from pions and deltas is of course most important at the highest bombarding energies.

If the unbound clusters are responsible for the difference in the extracted entropy at the lower bombarding energies then the disagreement should decrease with increasing bombarding energy, but this behavior is not seen in fig. 3b. The difference seen at the highest bombarding energy is probably too large to be explained by the production of pions and deltas which is not included in the model of Kapusta [7].

If the contributions from quantum statistics, unbound resonances, heavy fragments, pions and deltas are turned off in the calculations by Stöcker [8] then the resultant entropy values agree very well with the ones obtained from the model by Kapusta [7]. It is, however, not clear which of the above mentioned effects contribute most to the difference in the extracted entropy values.

If the produced entropy stays constant during the expansion then it contains information on the equation of state which controlled the reaction. Without an observable for the density reached in the reaction one is forced to rely on models relating the bombarding energy to the density. In the nuclear fireball model [12] all available kinetic energy goes into thermalization and thus no compression or density increase is implied. This results, for a cluster freeze out density of $\rho/\rho_0 = 1$, in the entropy and temperature values

shown in figs. 4a and b as the dashed curves. (The choice of a lower freeze out density would result in even larger entropy values.) The fireball calculations were done following the model of ref. 8. As can be seen from the comparison with the entropy values extracted from the data by the Stöcker method [8] this fireball prediction without compression is much too large.

In the hydrodynamical model some of the available kinetic energy goes into compressional energy. Hydrodynamical calculations using an equation of state based on the relativistic mean field theory of ref. 17 show a very good agreement with the experimentally extracted entropy values using the method of ref. 8. The choice of the equation of state does not change the entropy production significantly as was pointed out by Stöcker et al [18]. (An assumption of a softer equation of state results in slightly larger entropy values.) To differentiate and determine more precisely the proper equation of state is not possible partly due to the systematic errors in the method of extrapolation to infinite matter. We emphasize the need for methods and models describing the finite size of nuclear systems, where our data are of higher precision. However, from fig. 4a it is clearly seen that compression has to be present to explain the produced entropy in the collision.

In addition to the extracted entropy, apparent temperatures have been determined from the proton spectra at 90 degrees in the center of mass system [13]. This introduces a further specification of the thermodynamical properties of the reaction zone, however, unfortunately without an improvement in the knowledge of the density reached in the collision. The comparison between the temperatures from the calculations described above and the experimentally determined apparent ones is shown in fig. 4b. The latter ones

are the values extracted at maximum charged baryon multiplicity. The dashed curve is the result of the fireball calculation without compression and is close to the observed maximum apparent temperatures. The solid curve represents the temperature predicted from the hydrodynamical calculation using an equation of state based on the relativistic mean field theory of ref. 17, but without pions included.

Conclusions:

We have presented data on composite particle production as a function of multiplicity for different colliding systems and energies. These data can be understood by the improved coalescence model taking the radius and temperature of the participant region, as well as the radius of the deuteron into account. The obtained radii for the interacting volume give chemical freeze out densities between 50 and 100% of normal nuclear density. We have also presented results on entropy production in the systems studied by considering two different models for the determination of the entropy. The results show large differences which clearly show that the determination of entropy produced in nuclear collisions is strongly model dependent. Favoring the model by Stöcker [8] we conclude that compression is achieved in the collision and that the normal no-compression fireball model produces too much entropy. Thus the globally measured d/p ratios together with a proper method for the entropy determination allows one in principle to distinguish between different equations of state. A determination of the proper equation of state from data, however, would be improved by a model which does not need to extrapolate from the finite size volumes in nuclear collisions to that of infinite matter,

but rather uses the higher accuracy of the experimental data themselves. The findings that compression is needed to explain the entropy values can be related to the pressure effect observed in form of collective flow (side-splash) [19]. The flow phenomenon can now be connected with nuclear compression and not thermal pressure alone.

Acknowledgments:

We are grateful for the continuous support of Prof. R. Bock. H. Stöcker is acknowledged for performing the calculations referred to in this report and for many valuable and stimulating discussions. We also thank J. Boguta, M. Gyulassy and J. Kapusta for many very helpful suggestions. This work was supported in part by the Director, Office of Energy Research, Division of Nuclear Physics of the Office of High Energy and Nuclear Physics of the U.S. Department of Energy under Contract DE-AC03-76SF00098.

References:

1) H. Sato and K. Yazaki, Phys. Lett. 98B,153(1981)

2) A.Z. Mekjian, Phys. Rev. C17,1051(1978)

3) M. Gyulassy and E. Remler to be published

4) H.H. Gutbrod, H. Löhner, A.M. Poskanzer, T. Renner, H. Riedesel, H.G. Ritter, A. Warwick, F. Weik and H. Wieman, Phys. Lett. 127B,317(1983)

5) S.E. Koonin, Phys. Lett. 70B,43(1977)

6) P.J. Siemens and J.I. Kapusta, Phys. Rev. Lett. 43,1486(1979)

7) J.I. Kapusta, Phys. Rev. C29,1735(1984)

8) H. Stöcker, Nucl. Phys. A400,63c(1983) and B.V. Jacak, H. Stöcker and G.D. Westfall, Phys. Rev. C29,1744(1984)

9) G. Bertsch and J. Cugnon, Phys. Rev. C24,2514(1981)

10) J.I. Kapusta, Phys. Rev. C24,2545(1981)

11) A. Baden, H.H. Gutbrod, H. Löhner, M.R. Maier, A.M. Poskanzer, T. Renner, H. Riedesel, H.G. Ritter, H. Spieler, A. Warwick, F. Weik and H. Wieman, Nucl. Instr. Meth. 203,189(1982)

12) H.H. Gutbrod, A. Sandoval, P.I. Johansen, A.M. Poskanzer, J. Gosset, W.G. Meyer, G.D. Westfall and R. Stock, Phys. Rev. Lett. 37,667(1976)

13) H.-Å. Gustafsson, H.H. Gutbrod, B. Kolb, H. Löhner, B. Ludewigt, A.M. Poskanzer, T. Renner, H. Riedesel, H.G. Ritter, A. Warwick and H. Wieman, Phys. Lett. 142B,141(1984)

14) H.-Å. Gustafsson, H.H. Gutbrod, B. Kolb, H. Löhner, B. Ludewigt, A.M. Poskanzer, T. Renner, H. Riedesel, H.G. Ritter, A. Warwick and H. Wieman, Phys. Rev. Lett. 53,544(1984)

15) G. Fai and J. Randrup, Nucl. Phys. A404,551(1983)

16) H. Stöcker, Nucl. Phys. A418,587c(1984)

17) J. Boguta and H. Stöcker, Phys. Lett. 102B,289(1983)

18) H. Stöcker, M. Gyulassy and J. Boguta, Phys. Lett. 103B,269(1981)

19) H.-Å. Gustafsson, H.H. Gutbrod, B. Kolb, H. Löhner, B. Ludewigt, A.M. Poskanzer, T. Renner, H. Riedesel, H.G. Ritter, A. Warwick, F. Weik and H. Wieman, Phys. Rev. Lett. 52,1590(1984)

Table 1: Temperatures used in the fits and the rms radii extracted using equation (1).

System	Energy (MeV/nucleon)	T (MeV)	r_o (fm)	r_d (fm)
Ca + Ca	400	50	1.13 ± 0.05	4.52 ± 0.37
Ca + Ca	1050	85	0.92 ± 0.06	3.79 ± 0.47
Nb + Nb	400	50	1.16 ± 0.05	4.83 ± 0.56
Nb + Nb	650	70	1.00 ± 0.06	4.34 ± 0.69

Table 2: The asymptotic $(d_{like}/p_{like})_{asymp}$ values and the entropy per nucleon (S/A) for the different systems extracted by using the two models described in the text. The values are determined using the fit parameters from Table 1. Given is also the ratios at maximum charge baryon number $(d_{like}/p_{like})_{max}$.

System	Energy (MeV/nucleon)	$(d_{like}/p_{like})_{asymp}$	$(d_{like}/p_{like})_{max}$	S/A (Kapusta)
Ca + Ca	400	0.94 ± 0.12	0.53 ± 0.04	4.20 ± 0.25
Ca + Ca	1050	0.80 ± 0.16	0.45 ± 0.03	4.35 ± 0.25
Nb + Nb	400	0.99 ± 0.13	0.68 ± 0.05	4.15 ± 0.20
Nb + Nb	650	0.95 ± 0.17	0.62 ± 0.05	4.20 ± 0.25

System	Energy (MeV/nucleon)	S/A (Stöcker)
Ca + Ca	400	2.25 ± 0.50
Ca + Ca	1050	2.65 ± 0.50
Nb + Nb	400	2.40 ± 0.35
Nb + Nb	650	2.60 ± 0.50

Figure Captions:

Fig. 1: Schematic view of the Plastic Ball/Wall spectrometer.

Fig. 2: d_{like}/p_{like} as a function of proton multiplicity (N_p) for the two systems Ca + Ca at 400 and 1050 MeV/nucleon and Nb + Nb at 400 and 650 MeV/nucleon. The curves shown are from fits to equation (1).

Fig. 3: a) Chemical freeze out densities and b) Entropy per nucleon (S/A) as a function of bombarding energy for the two systems Ca + Ca at 400 and 1050 MeV/nucleon (filled points) and Nb + Nb at 400 and 650 MeV/nucleon (open points). The smaller error bars are from statistics only while the bigger ones also include the contributions from systematic errors.

Fig. 4: a) Entropy per nucleon (S/A), extracted using the model of Stöcker [8] and b) The experimentally determined apparent temperatures at maximum proton multiplicity as a function of bombarding energy (the symbols have the same meaning as in fig. 3). The solid and dashed curves are results of a hydrodynamic and a fireball calculation, respectively (see text for details).

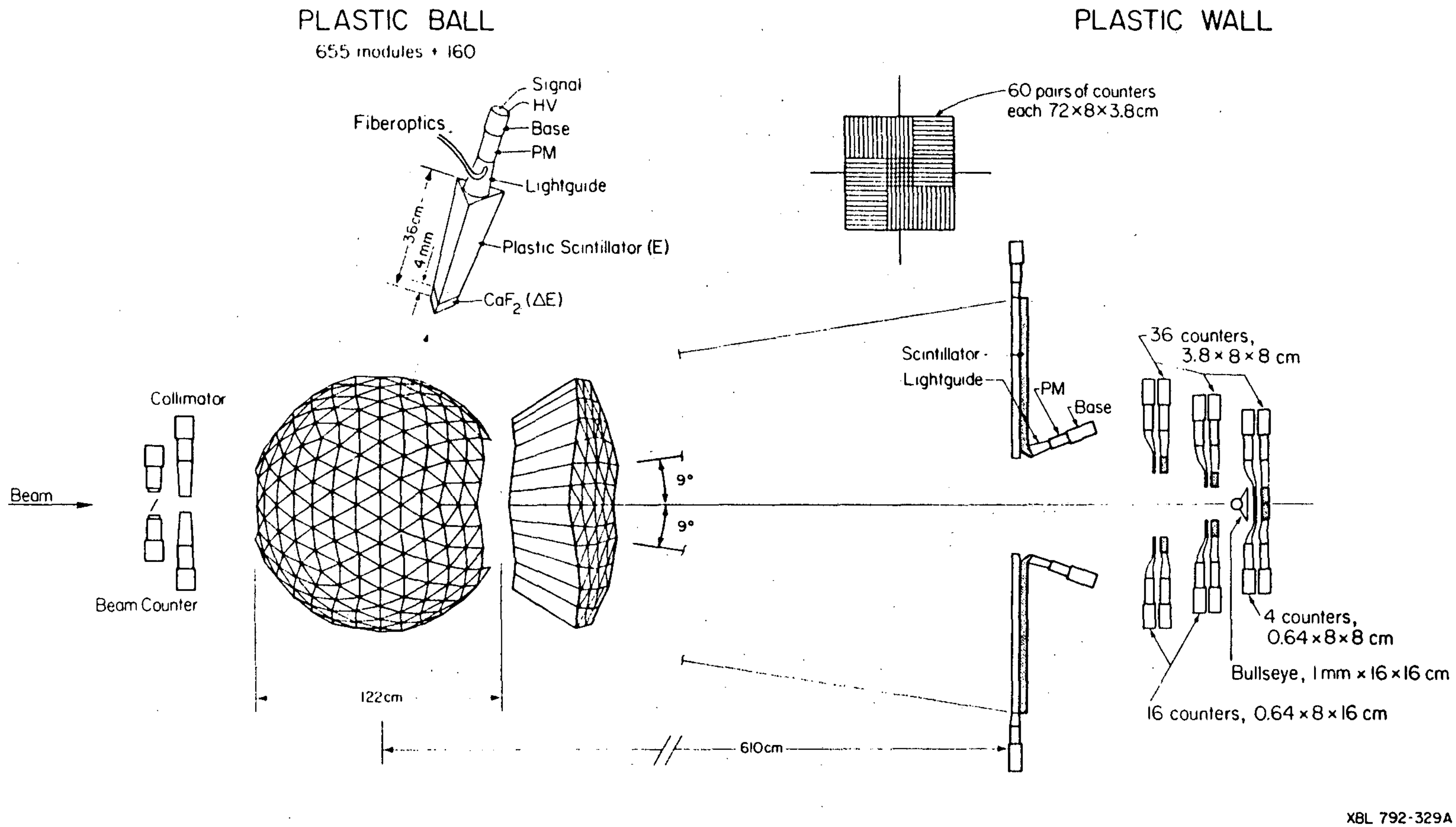
PLASTIC BALL
655 modules + 160
Signal
HV
Base
PM
Fiberoptics
Lightguide
36cm
4mm
Plastic Scintillator (E)
CaF2 (ΔE)
PLASTIC WALL
60 pairs of counters
each 72×8×3.8cm
Collimator
Beam
Beam Counter
9°
9°
122cm
610cm
Scintillator
Lightguide
PM
Base
36 counters,
3.8×8×8 cm
4 counters,
0.64×8×8 cm
Bullseye, 1mm×16×16 cm
16 counters, 0.64×8×16 cm
XBL 792-329A

Fig. 1

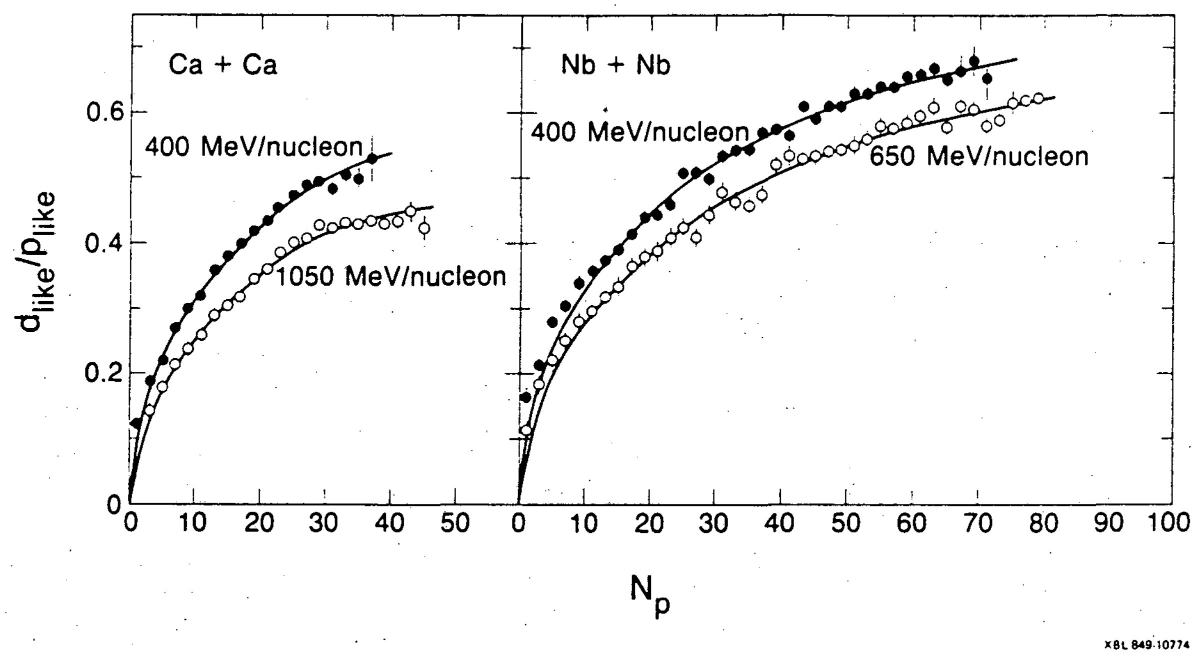

Ca + Ca
400 MeV/nucleon
1050 MeV/nucleon
Nb + Nb
400 MeV/nucleon
650 MeV/nucleon
d_like/p_like
0
0.2
0.4
0.6
0 10 20 30 40 50
0 10 20 30 40 50 60 70 80 90 100
N_p
XBL 849-10774

Fig. 2

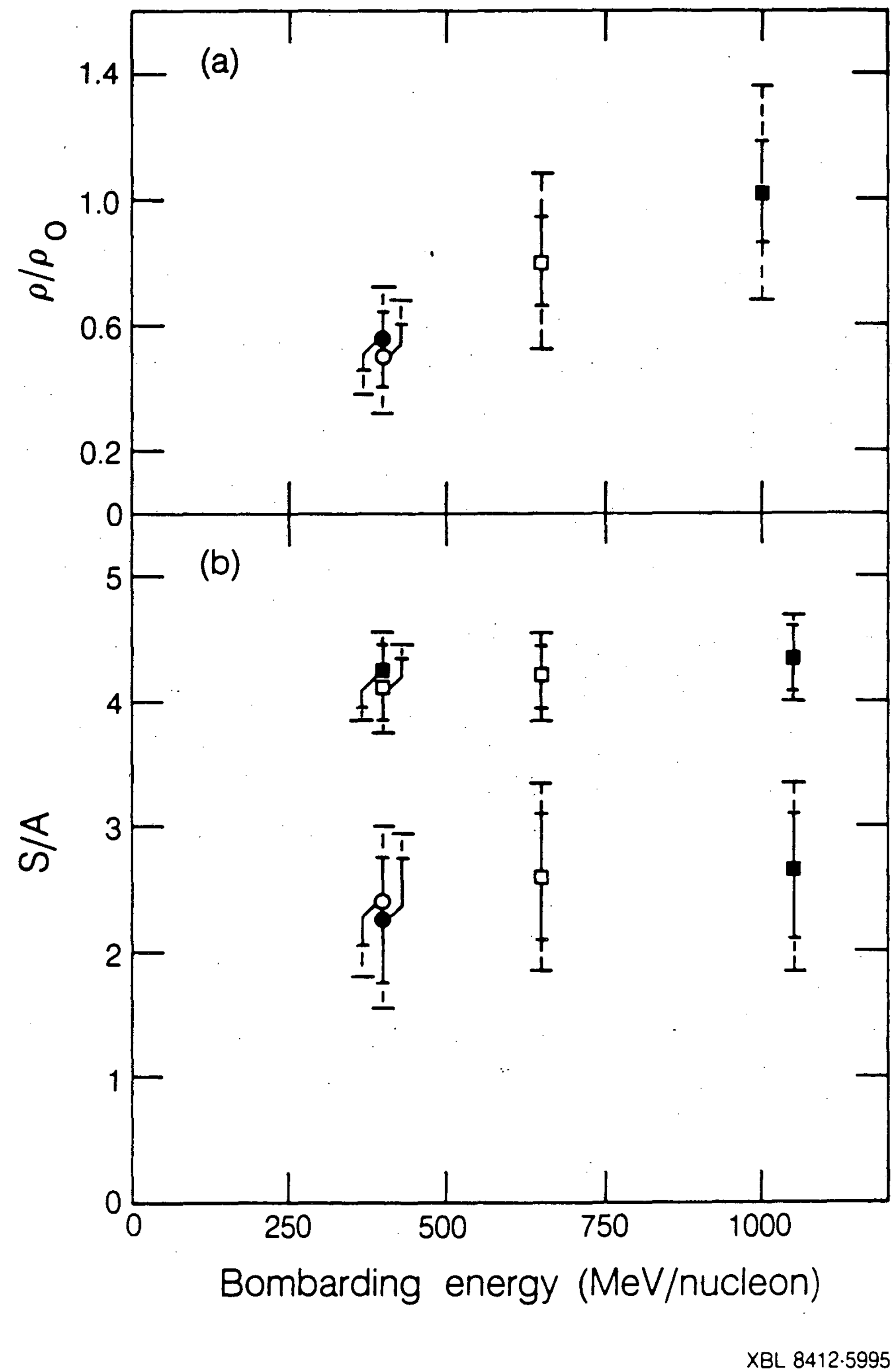
(a)
(b)
1.4
1.0
0.6
0.2
0
ρ/ρ_0
5
4
3
2
1
0
S/A
0
250
500
750
1000
Bombarding energy (MeV/nucleon)
XBL 8412-5995

Fig. 3

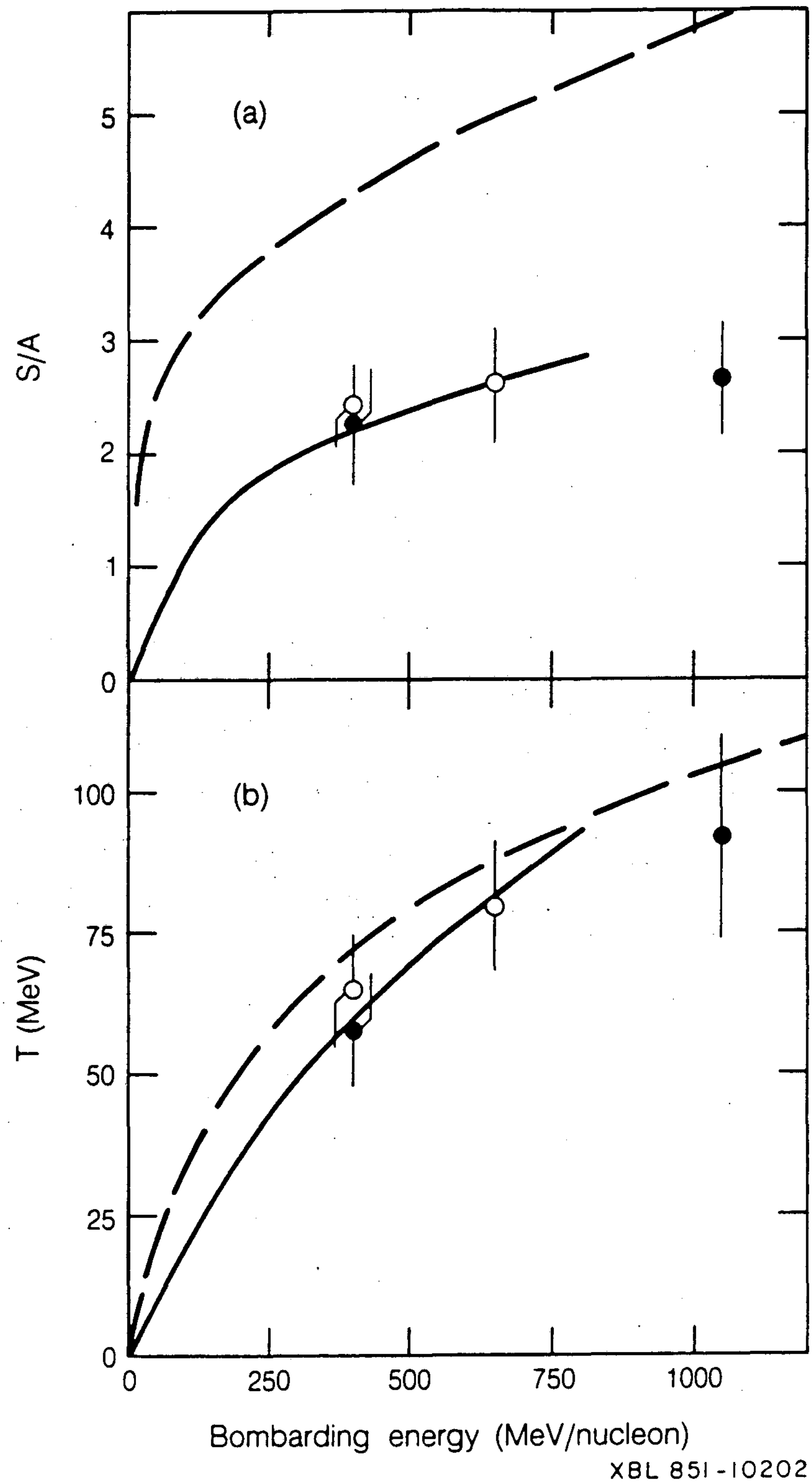
(a)
S/A
0
1
2
3
4
5
(b)
T (MeV)
0
25
50
75
100
0
250
500
750
1000
Bombarding energy (MeV/nucleon)
XBL 851-10202

Fig. 4

TECHNICAL INFORMATION DEPARTMENT
LAWRENCE BERKELEY LABORATORY
UNIVERSITY OF CALIFORNIA
BERKELEY, CALIFORNIA 94720